Mexnext-II: The Latest Results on Experimental Wind Turbine Aerodynamics

K. Boorsma and J.G. Schepers
Energy Research Centre of the Netherlands, ECN, P.O. Box 1, 1755 ZG Petten, The Netherlands
boorsma@ecn.nl

Sugoi Gomez-Iradi
National Renewable Energy Center, CENER, Pamplona, Spain

Helge Aagaard Madsen, Niels Sørensen and Wen Zhong Shen
Technical University of Denmark, DTU, Lyngby, Denmark

Christoph Schulz
Institute of Aerodynamics and Gasdynamics, University of Stuttgart, Stuttgart, Germany

Scott Schreck
National Renewable Energy Laboratory, NREL, Colorado, USA

Abstract

A selection of results from IEA Annex 29 Mexnext on analysis of wind tunnel measurements is presented. A convincing example illustrates the importance of detailed aerodynamic measurements. The influence of MEXICO blade shape deviations between design and manufactured geometry was assessed by scanning the blade geometry and performing comparative CFD simulations with this geometry. Generally speaking the differences between the results for design and scanned geometry do not justify the differences observed between experiments and computations A comparison between calculations and unexplored measurements from the famous NREL UAE PHASE VI experiment at a relatively high rotational speed is performed. It was found that as long as prescribed airfoil data is used, a good agreement exists between lifting line code results. The tip effect remains difficult to predict, although it is questioned in how far the limited blade aspect ratio is representative for large commercial wind turbines. CFD RANS simulations generally perform better in this respect, although separated flow features remain a challenge for these models as well. Preparations for a second experiment on the existing MEXICO test rig are discussed. New configurations will be tested and new apparatus including an acoustic array will be used, by which an even higher quality data set can be assured than the first data set. A standstill test of the MEXICO blades in the Delft Low speed tunnel allowed to determine an appropriate roughness configuration and to make sure that the blades and their data acquisition are in good shape for the New MEXICO campaign.

Keywords: Rotor aerodynamics, measurements, predictions

1 Introduction

The subject of aerodynamics is extremely important in wind energy. It does not only determine the energy production of a wind turbine, but it also determines the loads, stability, and noise of a wind turbine and not to forget the wake behind the turbine and the consequent wind farm losses. As such a thorough understanding of the detailed wind turbine aerodynamics is of crucial importance. The present paper describes the latest results from Mexnext [1], a large joint international project in which 19 parties from 9 countries cooperate in understanding the wind turbine aerodynamic behaviour using advanced aerodynamic measurements. The experiments herein range from a wide variety of sources, including measurements at the Japanese Mie university [2], the Chinese CARDC [3] and old FFA measurements [4]. Firstly the importance of sufficient detail in measurements is illustrated in section 2. One of the outcomes as discussed in section 3 deals with the influence of deviations between design and manufactured blade shape. Section 4 shows a comparison between measurements and calculations based on the NREL UAE PHASE VI experiment

[5]. Finally the preparations for a new MEXICO experiment [6] are discussed in section 5, followed by the conclusions.

2 Importance of detailed measurements

Two of the most representative wind tunnel experiments featuring relative large diameter and extensive instrumentation are the MEXICO and NREL UAE PHASE VI experiments. Both MEXICO and NREL UAE PHASE VI feature 5 instrumented radial sections with pressure sensors. Both experiments feature a Horizontal Axis Wind Turbine (HAWT), where the first is a 4.5 m diameter 3-bladed upwind rotor and the second a 2-bladed 10 m diameter upwind rotor (for most configurations). The need for this extensive instrumentation is illustrated in Figure 1, which shows a comparison between measured and predicted normal force distribution for the MEXICO turbine in axial flow conditions. Here the predictions are made using a blade element momentum (BEM) and a RANS Computational Fluid Dynamics (CFD) code and the measurement results are obtained by integrating sectional pressure distributions over the chord. The legend indicates that there is an excellent agreement in rotor axial force, which for this example is obtained by integration the sectional forces over the span. Hence, without any further information on the local aerodynamic loads this would indicate a good quality of the prediction code. However the availability of measured local aerodynamic loads made it possible to assess the agreement on a local level which showed a very poor performance of the BEM code. As illustrated, the good agreement in rotor axial force is misleading and caused by compensating errors only. Since the operating angle of attack for the mid- to outboard section is in the separated flow region for this case, it is questionable whether the BEM approach using 2D airfoil data is still applicable. Although the CFD code performs better on a local level, the agreement of the rotor integrated loads is less good in comparison to the measured values.

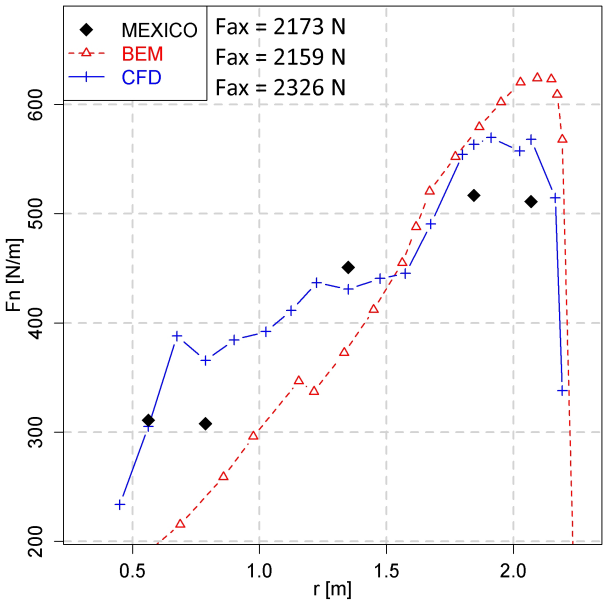

Figure 1: Radial distribution of sectional normal force, MEXICO turbine (U_∞=24 m/s, 424 rpm, -2.3 $^\circ$ pitch)

3 Influence of blade shape deviations

In a first phase of Mexnext several comparisons were made between measurements and calculations. In order to understand some of the differences it was considered important to know the actual blade shape and to compare it with the specified (design) shape. Thereto all three blade shapes have been scanned digitally. Comparing the geometries generally yielded some small differences [7], the most important quantities dictating the aerodynamics being the profile shape and twist angle. Nevertheless a CFD investigation (RANS simulations) from the Mexnext partners CENER and University of Stuttgart showed some non-negligible differences [8], see also Figure 2(a) for a grasp of the results. Hereto it should be realized that the measured loading originates from the five different instrumented sections that were distributed over the three blades. This means that the CFD results of the scanned geometry (`_SCANNED`, dashed lines) were taken from blade 1 for the inner part (25%R and 35%R), from blade 2 for the midboard part (60%R) and from blade 3 for the outboard part (82%R and 92%R). The results from CENER and University of Stuttgart are compared to the experimental data (black diamonds) and to their CFD results of the design geometry (solid lines). Although these simulations indicate small differences between the results for the scanned and design geometry (roughly $\pm$ 5% in normal force), these differences are smaller and sometimes in opposite direction compared to the over prediction of the design geometry CFD compared to the experimental data (around 15% in normal force). Therefore it is concluded that a blade geometry deviation can not solely be held responsible for the shown over prediction in comparison to the measurements.

Figure 2(b) zooms in on the differences between the three blades, which are more pronounced towards the outboard sections. It is expected that geometric differences at these sections stand out more easily due to the higher dynamic pressure. It appears that the blade 1 results often show an offset in comparison to blade 2 and 3, which is in contradiction with the geometry comparison [7] that reported the shape of blade 3 to deviate the most in comparison to the other blades. It is also noted that phase locked velocity measurements using PIV from the same experiment revealed an excellent agreement between the induced flow fields directly downstream from blade 2 and 3. This could indicate that the deviations mainly impact the loads directly but not so much the underlying flow field.

To judge the value of these differences it should be realized that to perform a CFD simulation from scanned geometry, the measured cloud of points must be converted to a surface geometry consisting of curves (usually an IGES file). This conversion process can be done in many different ways and the resulting curves are often smoothed, thereby disregarding small scale irregularities. Therefore the accuracy of the resulting geometry actually used for the CFD prediction can be questioned. Nevertheless, the results give an indication of uncertainties due to geometry differences between design and actual blade geometry.

4 Comparison between measurements and calculations

An extensive comparison between measurements and calculations on the MEXICO campaign was previously reported [1], where in addition to loads also velocities and lifting line variables (e.g. angle of attack) for both axial and yawed flow conditions were subject of investigation. It is however not only the MEXICO measurements which are used in the comparison but a main aim of Mexnext-II is also to consider other experiments. Thereto a new comparison round is defined on the NREL UAE PHASE VI experiment [5] at a rotational speed of 90 rpm. Even though the NREL UAE PHASE VI experiment has been used in many validation cases before [9], the rotor speed was usually only 72 rpm where the cases at 90 rpm remained unexplored. A summary of the cases under investigation is given in Table 1.

4.1 Description of codes and measurements

Most of the codes used in the current investigation are described in the final report of Mexnext-I [1]. A brief description of the experiment itself and the codes is given below. For the lifting line codes used, two calculation rounds were performed; one with prescribed 2D airfoil data and one with 3D corrected airfoil data. The latter can be distinguished by the extension of _3D in the legend name of each dataset. The 3D corrections used therefore are described below as well.

Table 1: NREL UAE PHASE VI comparison cases (axial flow)

Case	U_∞ [m/s]	Pitch angle [°]	Rot. speed [rpm]	α@80%R‡ (estimate) [°]	a† (estimate) [-]
I5	5.08	0	71.7	4.5	0.21
X5	5.02	3	90.2	1.5	0.20
X10	10.04	3	90.9	8.0	0.15
X12	12.02	3	91.6	10.0	0.11

‡ Angle of attack

† Rotor averaged axial induction factor

4.1.1 NASA-AMES

The comparison features a 2 bladed turbine with a 10 m rotor in upwind configuration without cone and tilt, placed in the large test section of the NASA-AMES wind tunnel. More details can be found in [5]. To obtain normal and tangential force (defined normal and parallel to the chordline respectively), the measured pressures are integrated over the chord by applying linear interpolation. The pressure value taken for each sensor is time averaged over the relevant datapoint. Axial force is obtained by linear interpolation of these forces over the span using the 5 instrumented sections, assuming zero load at the root and tip.

4.1.2 DTU_BEM

This code features BEM theory, where drag is included in the axial and tangential momentum balances and the Prandtl tip factor is applied to the induced velocities. To further correct the tip effects between 2D and 3D airfoil data, the tip loss factor is applied on the force obtained by applying 2D airfoil data. More details can be found in [10]. The 3D airfoil data caused by rotation is derived from the 2D airfoil data and the corrections are made in 3 regions of angles of attack, roughly to be the attached flow region until maximum lift, post stall and past leading edge separation. The coefficients that are needed to perform the correction are predetermined, i.e. they are derived prior to the calculation.

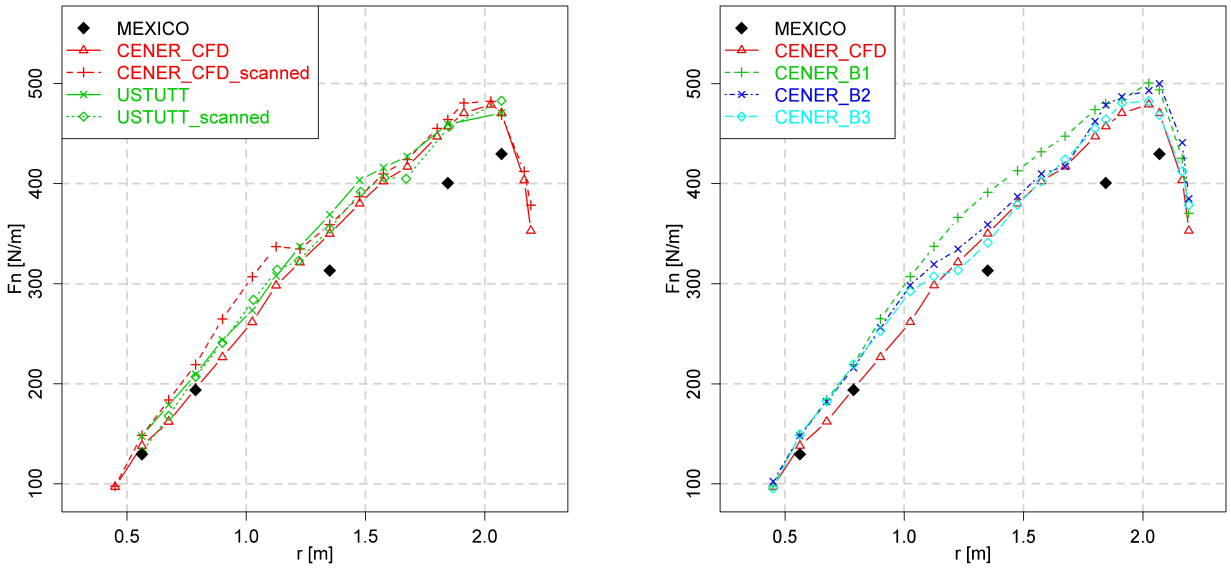

(a) Design and scanned geometry

(b) Individual blades

Figure 2: Radial distribution of sectional normal force, MEXICO turbine (U_∞=15 m/s, 424 rpm, -2.3 ° pitch)

4.1.3 DTU_HAWC2

The code is based on the BEM theory but extended from the classical approach to handle dynamic inflow, dynamic stall, skewed inflow, and shear effects on the induction [11]. There is no general 3D correction model included in the software but the airfoil input data are corrected, based on general experience with 3D effects and in particular the field rotor experiments at the former RISØ and at NREL [12, 13]. These main effects are a strongly delayed stall on the inner part of the blade, but also with a strong increases in drag. In addition to that there is some increase of the lift coefficient in post stall so that there is little or no negative slope on the lift curve in this region.

4.1.4 ECNAero

The ECN AERO-MODULE [14] includes both BEM as well as a lifting line free vortex wake formulation, allowing the same external input (e.g. wind, tower, airfoil data) to be used for both models. The BEM formulation is based on PHATAS [15], including state of the art engineering extensions which have matured over decades of research in wind turbine rotor aerodynamics. The free vortex wake method is based on the AWSM code [16]. The 3D correction is based on the model of Snel [17] as modified in PHATAS, dependent on chord over radius and tip speed ratio. As such it is embedded in the overall code, applied during the calculation and restricted to the inboard region below 50 ° angle of attack.

4.1.5 CENER_CFD

The Wind Multi-Block (WMB) code is used as developed by University of Liverpool and CENER [18]. The compressible Reynolds Averaged Navier-Stokes (RANS) flow equations are solved on multiblock structures grids using a cell-centred finite volume method for spatial discretization. The $k-\omega$ SST turbulence model of Menter is used. The geometry has been self-defined based on airfoil shape and blade planform table, featuring a sharp trailing edge.

4.1.6 DTU_EllipSys3D

The EllipSys3D code is a multiblock finite volume discretization of the incompressible RANS equations in general curvilinear coordinates [19]. The simulation includes transition computations based on the $\gamma - Re_\Theta$ correlation based transition model of Menter and turbulence modelling using the $k-\omega$ SST turbulence model of Menter. The geometry is based on a purposely developed IGES file as distributed within the Mexnext group, which features a finite trailing edge thickness.

4.2 Results

A selection of results is displayed in Figure 3. Judging by the axial force results in Figure 3(a), the results are generally in good agreement with each other and the experiment for the first two cases featuring attached flow conditions on the blades. This was confirmed by inspection of the radial distribution of normal force along the blade.

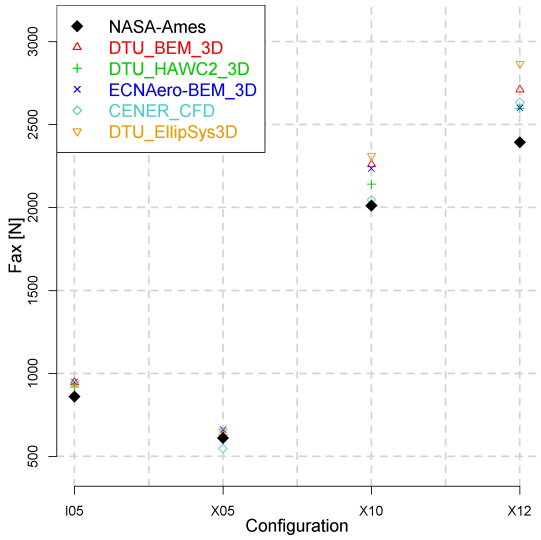

(a) Axial force for the different cases

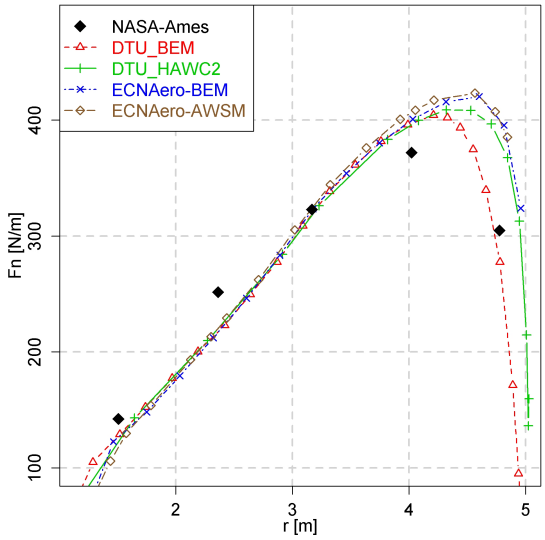

(b) Normal force, X10, 2D airfoil data

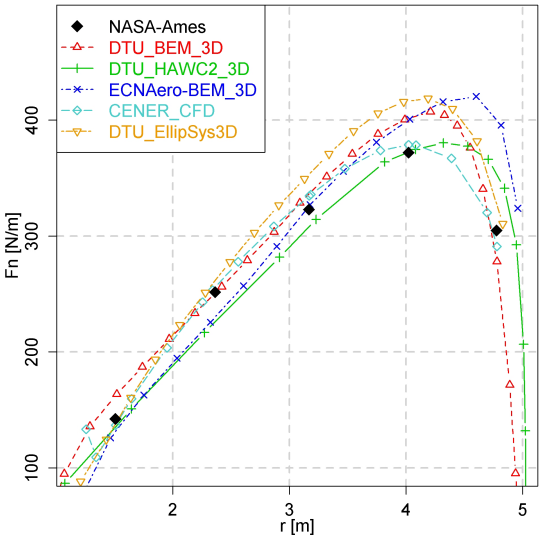

(c) Normal force, X10, 3D airfoil data and CFD

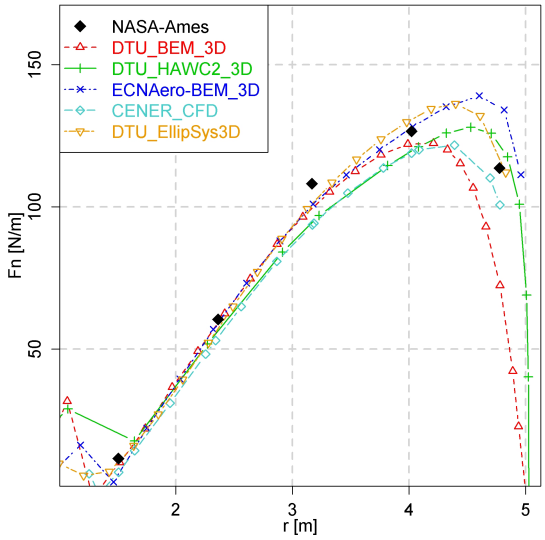

(d) Normal force, X5, 3D airfoil data and CFD

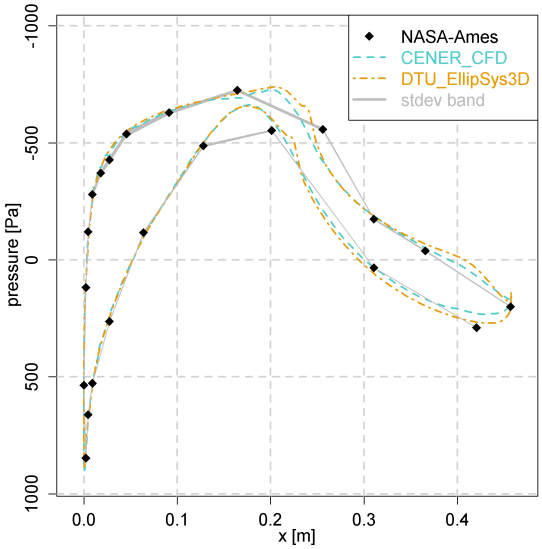

(e) Pressure distribution, X5, 80%R

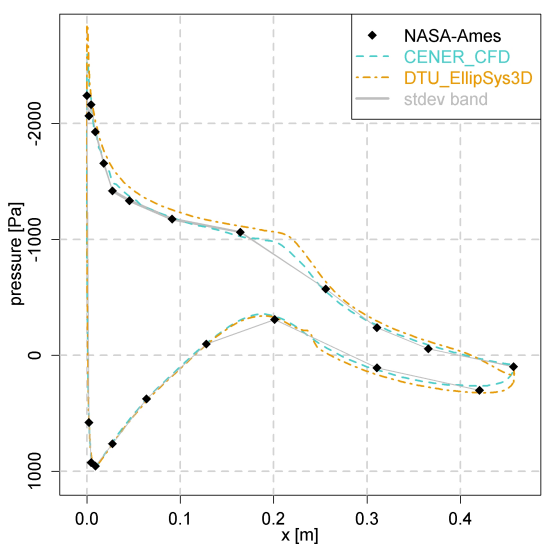

(f) Pressure distribution, X10, 80%R

Figure 3: Comparison between measurement and predictions, NREL UAE PHASE VI experiment

There is an overprediction for both lifting line codes as well as CFD for the X10 and X12 cases featuring separated flow conditions. Zooming in on the lifting line results with prescribed airfoil data for the X10 case in Figure 3(b), shows excellent agreement between predicted and measured values below 80%R. It is noted that a previous comparison round on this experiment [9] displayed a wide variation between predictions, possibly due to the differences in airfoil data used. In addition to that it can be observed that the tip correction model of DTU_BEM yields different results than the corrections used in DTU_HAWC2, ECNAero-BEM and ECNAero-AWSM. Vortex theory (ECNAero-AWSM) delivers the same result as the conventional Prandtl tip factor for this case, probably because the turbine is lightly loaded at an axial induction factor around 0.15. However, the differences in tip loading between ECNAero-BEM and ECNAero-AWSM remain relatively small also for the other cases. This indicates that the dominating tip effect is not the difference between local and annulus averaged induction but rather the lift fall-off due to the finite blade radius, which is expected to be more present for low aspect ratio rotors in comparison to modern turbines.

Application of 3D corrections and also including the CFD results then yields Figure 3(c). Here the spreading between the results increases and it can be observed that the DTU_HAWC2 3D correction is also applied to the outboard region of the blade. Overviewing all the cases, the currently applied 3D corrections mostly affect the X10 and X12 case since they exhibit separated flow along the span.

The CFD results are not in good agreement with each other, also not for the X5 case (Figure 3(d)), which could well be attributed to the different geometry used as addressed in section 4.1. The pressure distributions for these cases (Figure 3(e) and 3(f)) reveal differences in suction level and peak (X10) and slight 'kinks' in the DTU_EllipSys3D X5 upper and lower side pressure distribution aft of x=0.2 m due to boundary layer transition. The measured pressure distribution from the inevitable finite number of sensors just miss the bend in the pressure distribution around the maximum airfoil thickness. An estimate of the effect of the limited experimental chordwise and spanwise resolution was obtained by application of this resolution to the CFD results in the data reduction procedure and compare this to the results obtained with the original resolution. The influence of the limited spanwise resolution is found to be responsible for half the discrepancy in axial force between measurements predictions for the X10 and X12 case, while the agreement for the I5 and X5 case remains good due to the low absolute differences. On a relative scale, the finite number of pressure sensors in chordwise direction are responsible for a 10% decrease of normal force at 80%R for the X5 case, whereas this effect is found to be negligible for large angles of attack (X10 and X12 case).

5 New MEXICO experiment

The first MEXICO measurements led to various insights on the added value of CFD, on modeling improvements (e.g. tip effects, 3D-effects, yawed flow) and it led to an enhanced understanding of the 3D-flowfield around wind turbines [1]. Still the analysis of the first MEXICO measurements led to some open questions which need to be answered in a new experiment: MEXICO was the first experiment in which the detailed pressure distribution as well as the underlying flow field was measured but the relation between the two opposed the momentum relations (at least at design conditions). Consequently the relation between velocities and load needs further attention. Moreover some results suffered from data uncertainties and faulty instrumentation and some parts of the database (e.g. the measurements on dynamic inflow and standstill) were considered incomplete. A further motivation for New MEXICO are the enhanced PIV capabilities from DNW which became available recent years, where in particular the resolution and/or the size of the PIV sheets is increased leading to a much more complete mapping of the flow field. Further flow visualization is planned by application of oil to the blade surface and smoke candles from the blade tips. In addition to that, the acoustic noise sources will be measured with an acoustic array in order to establish the acoustic-aerodynamic link. Several new test cases will be added as well, such as the application of Guerney flaps and fast pitching actions.

5.1 Non rotating test

In preparation for this test the blades were placed in the TUDelft Low Speed Tunnel. In addition to checking the status of the blades and its instrumentation, this test also enabled the measurement of quasi-standstill sectional characteristics. Since this experiment finished very recently, much of the data analysis still needs to be performed and the here shown results are preliminary. The tunnel features an octagonal cross section of 1.25 m high by 1.8 m wide, in which the blades are positioned vertically pointing downward. Since the blade length of 2.04 m exceeds the tunnel height two configura-

(a) Inboard set-up (b) Outboard set-up

Figure 4: Test set-up in the Delft tunnel

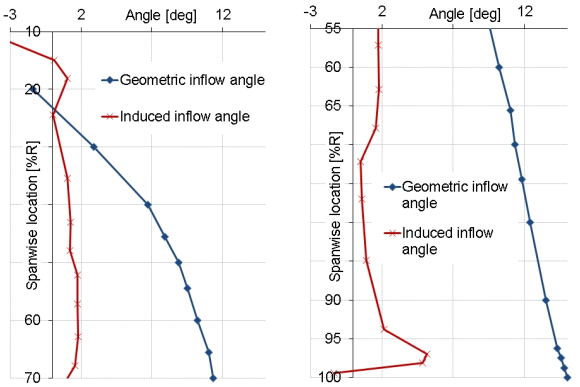

(a) Inboard set-up (b) Outboard set-up

Figure 5: Calculated induced angle of attack variation for a geometric tip angle of 15 °

tions were employed, one focusing on the outboard part (with a free tip) and one on the inboard blade part (with the tunnel floor cutting off the 69%R section), see also Figure 4. With a maximum tunnel speed of 100 m/s, the Reynolds numbers of the rotating experiment could be matched.

The data acquisition and pressure sensors were brought back to life successfully after an inactive period of more than seven years. Having a close look at the apparatus allowed for fixing some of the pressure signals in the inboard sections which were faulty during the first MEXICO campaign. A wake rake was positioned downstream of the blade to measure the velocity deficit. In addition to obtaining sectional drag, traversing the rake along the blade span for all three blades gave a possibility to further investigate the agreement between the blades.

5.1.1 Sectional characteristics

Using the ECN AERO-MODULE free vortex wake code AWSM, a first survey was performed to investigate the angle of attack variation along the blade using prescribed airfoil data. By this approach an estimate of the degree of 'two-dimensionality' of the experimental set-up can be obtained. Although full details such as wall effects are not taken into account here, this approach yields an approximation for the order of magnitude of the induced velocities causing different inflow angles than the local geometric twist angle. The results shown in Figure 5 reveal that for this particular blade pitch angle induced angles of attack exceeding 2 ° can be expected, not only confined to the tip area. Hence the trailing vorticity is not only concentrated in the tip vortex but also plays a role in the remainder of the span due to the varying circulation along the blade span as a consequence of the radial twist and chord distribution. Increasing or decreasing the blade pitch angle from this value is found to reduce the induced velocities. For the 15 ° pitch angle, the geometric angle of attack along the blade in combination with the chord distribution results in a circulation distribution where the trailing vorticity is most effective in inducing velocities perpendicular to the chordline.

Although it is clear that the test set-up cannot be used to determine sectional characteristics directly, the set-up can be considered comparable to parked rotor conditions. Combining the measurements with a planned CFD simulation including the tunnel will possibly reveal information on the underlying two dimensional sectional characteristics.

5.1.2 Roughness strips and visualization

A stethoscope was traversed over the blade surface to determine the location of laminar to turbulent transition. In a clean configuration, small surface irregularities were found to dictate the chordwise position of transition along the span. This is regarded as unwanted taking into account comparison to CFD calculations. The minimum width (5mm) and thickness (0.2 mm) zigzag strip to yield transition for the range of angles of attack and Reynolds numbers was determined, to keep parasitic drag due to the strip itself to a minimum. The chordwise position of the strips was kept at 10%chord for both pressure and suction side of the blades. The zigzag strips positioning close to the pressure sensors were modified in such a way that distortion of the measured pressure distribution by local pressure changes due to the small vortices emanating from the zigzag shape was prevented.

An oil flow visualization in the set-up for the outboard part of blade 3 confirmed that the roughness strips indeed provoke transition. Figure 6(a) shows

laminar to turbulent boundary layer transition (directly aft of the zizag strip), illustrated by the light and respectively darker colours due to the different friction coefficient between them. The difference with the tip region which does not feature a zigzag strip is clearly noticeable. The tape covering the sensors at 60%R, 82%R and 92%R can be observed from top to bottom respectively. Due to the twist distribution, the geometric angle of attack is 4.8°, 2.4° and 1.2° larger for these sections respectively than the tip angle. Because of this the outboard sections already exhibit trailing edge separation, which can be observed by the bright colours due to the oil not being transported over the surface. Generally speaking the flow pattern can be considered two-dimensional. Figure 6(b) then shows a configuration at a higher tip pitch angle, where spanwise flow features can be observed in the separated flow region. In addition to that a small laminar separation bubble can be observed by a bright coloured line before the roughness strip just aft of the leading edge, approximately between the tip and 70%R. Figure 6(c) shows the lower side surface for a negative angle of attack, where the midboard part of the blade shows separation in the cusp of the RISØ profile.

6 Conclusions

In the Mexnext project detailed aerodynamic measurements are used. These measurements provide local aerodynamic loads along the blade where in addition the underlying flow field which drives these loads is mapped in some experiments. It is proven that such very detailed information is needed to better understand the aerodynamic behaviour of a wind turbine. With this better understanding it is possible to improve wind turbine design codes which eventually leads to more reliable and more efficient wind turbines. Furthermore the detailed measurements form essential and unique validation material for wind turbine design code by which the the validity of these codes can be assessed and which enables the identification of areas where improvement is needed. Much progress has been made in the project where measurements are used from a large variety of sources, mainly wind tunnel measurements but also field measurements. The paper puts emphasis on a comparison between calculations and unexplored measurements from the famous NREL UAE PHASE VI experiment at a relatively high rotational speed. Moreover results from the MEXICO measurements are shown and the differences are assessed between the measured and specified blade geometry including the effect of these differences on the loads. It is shown that much more work is needed. Thereto the so called New MEXICO experiment is performed, i.e. a second experiment on the existing MEXICO test rig in order to fill the missing gaps and to take into account the lessons learnt from the first MEXICO experiment. Hereby an even higher quality data set can be obtained compared to the data set from the first campaign.

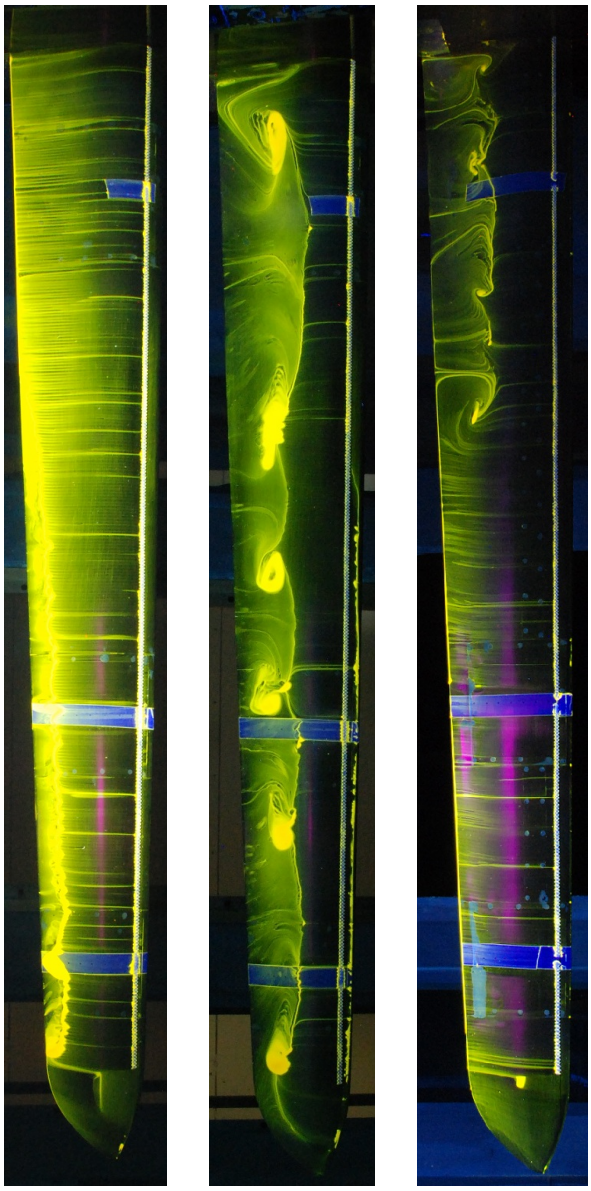

(a) 10.4° upper side (b) 16.4° upper side (c) -3.6° lower side

Figure 6: Blade oilflow visualization for a variety of geometric angles of attack referenced to the tip chord (flow from right to left), U_∞=60 m/s

References

[1] J.G. Schepers and K. Boorsma et al. Final report of IEA Task 29, Mexnext (Phase 1): Analysis of MEXICO wind tunnel measurements. ECN-E-12-004, Energy Research Center of the Netherlands, February 2012.

[2] Y. Kamada Y. and T. Maeda. Experimental Study on Velocity Field around Wind Turbine Rotor. *Japan Society Mechanical Engineering Journal*, 71(701), 2011.

[3] J. Xiao et al. Particle image velocimetry (PIV) measurements of tip vortex wake structure of wind turbine. *Applied Mathematics and Mechanics (English Edition)*, 32(6), 2011.

[4] G. Ronsten. Geometry and Installation in Wind Tunnels of a STORK 5.0 WPX Wind Turbine Blade Equipped with Pressure Taps. Technical Report FFA 1006, The Aeronautical Research Institute of Sweden, 1994.

[5] M.M. Hand et al. Unsteady Aerodynamics Experiment Phase VI Wind Tunnel Test Configurations and Available Data Campaigns. NREL/TP-500-29955, National Renewable Energy Laboratory, NREL, December 2001.

[6] J.G. Schepers and H. Snel. MEXICO, Model experiments in controlled conditions. ECN-E-07-042, Energy Research Center of the Netherlands, 2007.

[7] T.H. Cho. MEXICO Blade 3D measurement. In *Annual IEA Task 29 meeting presentations, Jeju Island, South Korea*, June 2011.

[8] K. Boorsma, S. Gomez-Iradi, and C. Schulz. On the influence of MEXICO blade shape deviations, Comparison of CFD results using scanned and design blade geometry. ECN-X–13-038, Energy Research Center of the Netherlands, April 2013.

[9] D.A. Simms S. Schreck M.M. Hand L.J. Fingersh. NREL Unsteady Aerodynamics Experiment in the NASA-Ames Wind Tunnel: A Comparison of Predictions to Measurements. NREL/TP-500-29494, The National Renewable Energy Laboratory, NREL, June 2001.

[10] W.Z. Shen et al. Tip Loss Corrections for Wind Turbine Computations. *Wind Energy*, 8(4), 2005.

[11] H. Aa Madsen et al. Validation and Modification of the Blade Element Momentum theory based on comparisons with actuator disc simulations. *Wind Energy*, 13(4), 2009.

[12] J. G. Schepers, A. Brand, A Bruining, J. Graham, M. Hand, D. Infield, H. Madsen, J. Paynter, and D. Simms. Final Report of IEA Annex XIV: Field Rotor Aerodynamics. Technical report, ECN-C–97-027, 1997.

[13] J. G. Schepers, A. Brand, A Bruining, M. Hand, D. Infield, H. Madsen, T. Maeda, J. Paynter, R. van Rooij, Y. Shimizu, D. Simms, and N. Stefanatos. Final Report of IEA Annex XVIII: Enhanced Field Rotor Aerodynamics Database. Technical report, ECN-C–02-016, 2002.

[14] K. Boorsma, F. Grasso, and J.G. Holierhoek. Enhanced approach for simulation of rotor aerodynamic loads. Technical Report ECN-M–12-003, ECN, presented at EWEA Offshore 2011, Amsterdam, 29 November 2011 - 1 December 2011, 2011.

[15] C. Lindenburg and J.G. Schepers. Phatas-IV aeroelastic modelling, release "dec-1999" and "nov-2000". Technical Report ECN-CX–00-027, ECN, 2000.

[16] A. Van Garrel. Development of a wind turbine aerodynamics simulation module. Technical Report ECN-C–03-079, ECN, 2003.

[17] H. Snel, R. Houwink, G.J.W. van Bussel, and A. Bruining. Sectional prediction of 3d effects for stalled flow on rotating blades and comparison with measurements. In *Proc. European Community Wind Energy Conference*, 1993.

[18] S. Gomez-Iradi, R. Steijl, and G.N. Barakos. Development and validation of a CFD technique for the aerodynamic analysis of HAWT. *Journal of Solar Energy, Engineering-Transactions of the ASM*, 131(3), 2009.

[19] N.N. Sørensen. General Purpose Flow Solver Applied to Flow over Hills. Technical Report RISØ-R-827-(EN), RISØ National Laboratory, 1995.

Acknowledgements

The authors would like to thank the participants of the Mexnext group for the pleasant cooperation. The EU Innwind project is acknowledged for financial support in preparing the new MEXICO experiment. Finally the DUWIND department of the TUDelft, in particular G.J.W. van Bussel, W.A. Timmer, Y. Zhang and D. Baldacchino, are acknowlegded for their support during the standstill test of the MEXICO blades in the Delft University low speed tunnel.